

# Adaptively Biased Output Cap-Less NMOS LDO With 19 ns Settling Time

Debashis Mandal<sup>ID</sup>, Chirag Desai<sup>ID</sup>, Bertan Bakkaloglu, *Fellow, IEEE*, and Sayfe Kiaei, *Fellow, IEEE*

**Abstract**—This paper presents an output external capacitor-less, fully integrated, fast settling NMOS low-dropout (LDO) regulator with adaptively biased error amplifier (EA) for system-on-chip core applications. The adaptive biasing technique increases both loop bandwidth and slew-rate of the LDO by 100% at full load condition without changing no-load quiescent current. Direct feedback to gate-to-source voltage of the NMOS regulation FET provides fast load transient response. The proposed LDO employs a cross-coupled common-gate input based EA, with transconductance boosting, achieving twice unity-gain bandwidth in comparison to a typical folded-cascode common-source input stage. Low output impedance of NMOS regulation stage and low input impedance of the EA reduce load dependent stability issue. The proposed regulator is designed and fabricated in a 0.18- $\mu\text{m}$  CMOS technology with die-area of 0.21 mm<sup>2</sup>. The LDO generates a regulated output voltage of 1.4–1.6 V from an input voltage of 1.6–1.8 V, consumes 133  $\mu\text{A}$  quiescent current, and supports 0 pF to 50 pF load capacitance. Measured results show 166 mV undershoot with 19 ns settling time for a load step from 9 mA to 40 mA in 350 ps edge-time for zero-load capacitance. After using adaptive biasing, the settling time is reduced by 37% and 36% for 0 pF and 50 pF load, respectively.

**Index Terms**—Adaptively biased error amplifier, NMOS low-dropout (LDO) regulator, cross-coupled common-gate input stage, fast load transient response, fast slew-rate.

## I. INTRODUCTION

**D**UE TO low output noise and fast load transient response, high performance linear low-dropout (LDO) regulators are indispensable for system-on-chip (SoC) dynamic voltage and frequency scaling (DVFS) core applications. Usually a large off-chip load capacitor ( $C_L$ ) in micro-Farad range is used at LDO output ( $V_{OUT}$ ) to get small output undershoot/overshoot and fast output voltage settling during load transients. The large  $C_L$  also improves LDO power supply rejection (PSR). However, due to a large area requirement,  $C_L$  in micro-Farad range is not integrated in SoC. This results

in a significant degradation of both PSR and load transient response (undershoot/overshoot and settling time) for the fully-integrated output external capacitor-less (OECL)-LDOs.

The output  $C_L$ , and the gate capacitor ( $C_G$ ) of regulation FET are two largest capacitors for an LDO. Hence, there are at least two low frequency poles: one located at the LDO output ( $\omega_{POUT}$ ), and other at the gate of regulation FET ( $\omega_{PG}$ ), where  $\omega_{POUT}$  is load current ( $I_L$ ) dependent. For a large off-chip  $C_L$ , LDOs are designed to be  $\omega_{POUT}$  dominant, and a large quiescent current ( $I_Q$ ) is burned to move  $\omega_{PG}$  to high frequency. However, OECL-LDOs are designed to be  $\omega_{PG}$  dominant, and such LDOs with limited on-chip  $C_L$  up to a few hundred pico-Farad are reported in [1]–[8]. In [9], to support a wide range of  $C_L$  at LDO output, an error amplifier (EA) based on current operational amplifier with input common-gate (CG) transistors is used.

To achieve a fast load transient response with a small or no on-chip load capacitor  $C_L$ , OECL-LDOs are required to be designed with a wide loop unity-gain bandwidth (UGB), and a faster slewing during load transient. The OECL-LDOs in [1]–[6] are designed with PMOS regulation FET. The smaller  $C_G$  of an NMOS regulation FET, compared to a PMOS FET, provides relatively high frequency  $\omega_{PG}$ , hence a wider loop UGB, and a faster slew-rate (SR) during load transient. Moreover, the source follower configuration of the NMOS regulation FET provides an inherent low output impedance, which reduces load dependent stability issues. Due to a direct feedback to gate-to-source voltage of the regulation FET, NMOS regulation FET LDO (NMOS LDO) gives a faster load transient response than the PMOS regulation FET LDO (PMOS LDO). Also, the NMOS LDO inherently provides better PSR.

To enhance the SR, an EA with input cross-coupled CG transistors and output current summing stage is implemented in PMOS LDO [3]. However, the load transient settling time of  $V_{OUT}$  is about 4  $\mu\text{s}$ , which is a quite large for DVFS applications. In [10], a linear voltage regulator based on cascode NMOS regulation FET is designed for minimum 1.67 V dropout voltage ( $V_{DROP}$ ) between input voltage ( $V_{IN}$ ) and  $V_{OUT}$ , hence it is not suitable for low dropout applications. A switched-capacitor step-down DC-DC converter with series NMOS LDO is presented in [7], where the input voltage of the converter is directly used as the supply voltage for the EA of LDO. For the NMOS LDO in [8], the maximum  $I_L$  is 1 mA. However, the  $V_{OUT}$  settling time during load transient is more than 300 ns in [7], and 10.4  $\mu\text{s}$  in [8], which are quite large for DVFS SoC applications. An OECL analog-assisted digital LDO (AA-DLDO) using output PMOS regulation switches is presented in [11], however its load transient  $V_{OUT}$  settling time is more than 3  $\mu\text{s}$ .

In this paper, a wide bandwidth OECL-NMOS LDO with adaptively biased EA is proposed that achieves 166 mV undershoot and 19 ns settling time for 4.5X load step in 350 ps edge-time for zero  $C_L$ . A wide bandwidth EA with

Manuscript received March 11, 2018; revised April 29, 2018; accepted May 21, 2018. Date of publication May 31, 2018; date of current version January 29, 2019. This work was supported in part by NXP Semiconductors, Chandler, AZ, USA, and in part by the Connection One Center, Arizona State University, AZ, USA. This paper was recommended by Associate Editor J. Goes. (Debashis Mandal and Chirag Desai contributed equally to this work.) (Corresponding author: Debashis Mandal.)

D. Mandal, B. Bakkaloglu, and S. Kiaei are with the School of Electrical, Computer, and Energy Engineering, Arizona State University, Tempe, AZ 85287 USA (e-mail: debashis.mandal@asu.edu).

C. Desai was with the School of Electrical, Computer, and Energy Engineering, Arizona State University, Tempe, AZ 85287 USA. He is now with QCT PMIC Design, Qualcomm Technologies Inc., San Diego, CA 92121 USA.

Color versions of one or more of the figures in this paper are available online at <http://ieeexplore.ieee.org>.

Digital Object Identifier 10.1109/TCSII.2018.2842642

1549-7747 © 2018 IEEE. Personal use is permitted, but republication/redistribution requires IEEE permission.

See [http://www.ieee.org/publications\\_standards/publications/rights/index.html](http://www.ieee.org/publications_standards/publications/rights/index.html) for more information.

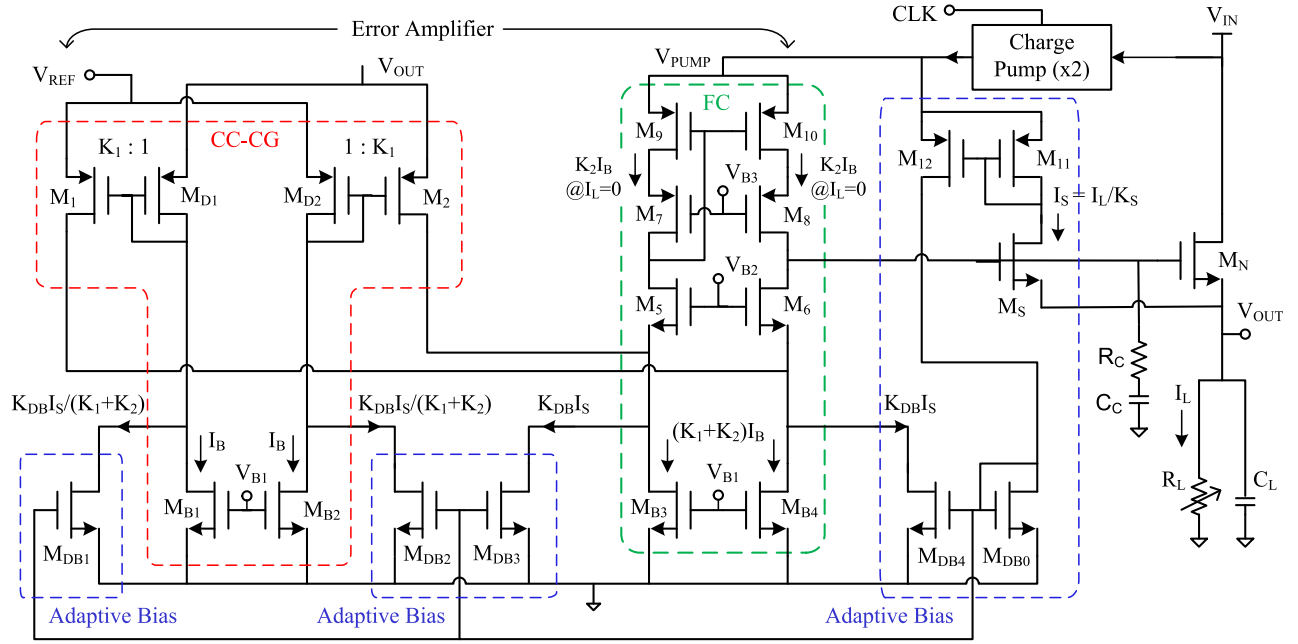


Fig. 1. Proposed NMOS regulation FET LDO with adaptive biasing.

a low input impedance and a high DC gain is designed using a cross-coupled (CC) CG input differential pair and a folded cascode (FC) output stage. The low input impedance of the EA further reduces LDO output impedance at no-load condition hence reduces the effect of output load variation on the LDO loop stability. The CC-CG input differential pair provides twice transconductance compared to a conventional CG stage with negligible increment of input bias current. Moreover, an adaptive-biasing circuit is designed to sense the regulation FET current, which enhances loop UGB and boosts the SR, hence, further improving the load transient response. A charge-pump voltage doubler (CPVD) in [12] is used to generate the supply voltage for the EA output stage to raise the gate voltage of NMOS regulation FET, ensuring the  $V_{DROP}$  of 200 mV across the regulation FET. The rest of this paper is organized as follows. The proposed LDO is discussed in Section II. Section III presents the loop stability analysis. Section IV summarizes the measurement results and Section V concludes this paper.

## II. PROPOSED LDO ARCHITECTURE

The schematic of the proposed NMOS LDO is shown in Fig. 1. It consists of an NMOS regulation FET ( $M_N$ ) at output, an error amplifier (EA), an adaptive biasing circuit (ABC), and a CPVD. The EA compares  $V_{OUT}$  with a reference voltage ( $V_{REF}$ ), generates the required gate drive voltage for  $M_N$ , and regulates  $V_{OUT}$  to  $V_{REF}$ . The EA is a FC-CG amplifier. The CG input stage provides a low input resistance of the EA. Thus, the direct feedback of  $V_{OUT}$  to the EA input maintains the low output resistance at quiescent mode of operation, hence stabilizing the regulation loop across a wide load range. High output resistance of the FC output stage sets the pole  $\omega_{PG}$  as the dominant pole of the system, and also provides high DC loop gain. The ABC improves  $V_{OUT}$  regulation during load transient and also improves loop UGB. Using clock (CLK) frequency of 20 MHz, two flying capacitors of 5 pF each, and an output capacitor of 30 pF, the CPVD generates  $2V_{IN}$  nominal supply voltage ( $V_{PUMP}$ ) of 3.4 V for the EA output stage from the  $V_{IN}$  of 1.8 V, to raise the gate voltage of the NMOS regulation FET above  $V_{IN}$ . By using a switching frequency of

20 MHz, the output ripple of CPVD is negligible, hence the output of the LDO is immune to the switching noise coupling through the EA and the  $C_{GS}$  of the NMOS regulation FET.

### A. Error Amplifier (EA)

Error amplifier is a folded cascode common-gate amplifier. Transistor pairs  $M_{D1}$ - $M_1$  and  $M_{D2}$ - $M_2$  are two transconductance ( $g_m$ ) stages at the input of EA. The source of  $M_1$  ( $M_2$ ) and source of diode-connected transistor  $M_{D1}$  ( $M_{D2}$ ) are the two inputs, and the drain of  $M_1$  ( $M_2$ ) is the output of the  $g_m$ -stage. The bias current of  $M_1$  ( $M_2$ ) is set  $K_1$  times of that of  $M_{D1}$  ( $M_{D2}$ ). Two such  $g_m$ -stages are cross-coupled to form differential input stage for the EA with a low input impedance. Due to the CC structure, twice input differential swing gets amplified, which provides twice the overall transconductance for the EA, enabling twice UGB with respect to a conventional FC-CS amplifier, and consequently twice the speed. Equivalent transconductance ( $G_{mEA}$ ) and single-ended input resistance ( $R_{IEA}$ ) of the EA are written as (ignoring transistor's output resistance),

$$G_{mEA} = 2g_{mI}, R_{IEA} \approx \frac{K_1}{(K_1 + 1)(g_{mI} + g_{mbI})} \quad (1)$$

where,  $g_{mI}$ ,  $g_{mbI}$  are transconductance, body-effect transconductance of transistor  $M_1$  or  $M_2$ , and  $g_{mI}/K_1$ ,  $g_{mbI}/K_1$  are transconductance, body-effect transconductance of  $M_{D1}$  or  $M_{D2}$ , respectively. The source terminals of transistors  $M_2$  and  $M_{D1}$  are directly connected to the output of the LDO.

The FC output stage, formed by transistors  $M_{B3}$ ,  $M_{B4}$ ,  $M_5$ - $M_{10}$ , provides a high output resistance at EA output, and high open loop DC gain. The output resistance ( $R_{OEA}$ ) of the EA is written as (ignoring transistor's body effect),

$$R_{OEA} = \frac{1}{\frac{1}{g_{mM8}r_{oM8}r_{oM10}} + \frac{(r_{oM1} + r_{oMB4})}{g_{mM6}r_{oM1}r_{oMB4}r_{oM6}}} \quad (2)$$

where,  $g_{mM6}$ ,  $g_{mM8}$ , are transconductance of  $M_6$ ,  $M_8$ ; and  $r_{oM1}$ ,  $r_{oMB4}$ ,  $r_{oM6}$ ,  $r_{oM8}$ ,  $r_{oM10}$  are output resistance of  $M_1$ ,  $M_{B4}$ ,  $M_6$ ,  $M_8$ ,  $M_{10}$ , respectively. The bias current

of current source transistors  $M_{B3}$  and  $M_{B4}$  is  $(K_1 + K_2)I_B$ . In quiescent mode of operation (i.e.,  $I_L = 0$ ), output current of adaptive bias circuit is negligible (i.e.,  $I_{MDB1} = I_{MDB2} = I_{MDB3} = I_{MDB4} = 0$ ), hence current through  $M_1$  or  $M_2$  is  $K_1 I_B$  and current through each output branch is  $K_2 I_B$ . The SR at the gate of regulation FET ( $SR_G$ ) is expressed as,

$$SR_G = \frac{(K_1 + K_2)I_B}{C_G} \quad (3)$$

Therefore, to support load current change in a very short time (a few hundred pico-second),  $SR_G$  is required to be large. This can be achieved by increasing the bias current  $(K_1 + K_2) I_B$ , which increases LDO quiescent current  $I_Q$ .

### B. NMOS Regulation FET

The smaller  $C_G$  of NMOS regulation FET, compared to the PMOS FET, moves the dominant pole  $\omega_{PG}$  to higher frequency, hence a wider loop UGB and a fast SR are achieved, improving the load transient response (undershoot/ overshoot and settling time) as well as the PSR. The low output resistance due to the source follower configuration of NMOS regulation stage maintains a good loop stability over a wide  $I_L$  range. The equivalent output resistance of the LDO is expressed as,

$$R_{OUT} = \frac{1}{[(g_{mMN} + g_{mbMN} + \frac{1}{r_{oMN}}) + \frac{1}{R_{IEA}}] + \frac{1}{R_L}} \quad (4)$$

where,  $g_{mMN}$ ,  $g_{mbMN}$ ,  $r_{oMN}$  are transconductance, body-effect transconductance and output resistance of  $M_N$ . DC voltage gain of the output regulation stage is  $g_{mMN} R_{OUT}$ , with a maximum value of unity. At light-load this gain is less than unity, and it reaches close to unity at full-load condition.

### C. Adaptive Biasing

A typical digital current load in a DVFS system includes thousands of gates turning on in a very short time (in order of few hundred pico-seconds). Consequently, there is a significant undershoot at  $V_{OUT}$ . The LDO needs to react, and settle the  $V_{OUT}$  to its steady state value, quickly. Employing adaptive biasing technique, as the load changes EA bias current increases, which improves  $SR_G$ , hence the LDO load transient response.

In Fig. 1, the transistor  $M_S$  is placed in parallel with the output regulation FET  $M_N$ , which senses a fraction  $(1/K_S)$  of  $I_L$  flowing through  $M_N$ . This sensed current ( $I_S$ ) is mirrored by a transistor pair  $M_{11}$ - $M_{12}$  and fed to the EA through transistors  $M_{DB0}$ ,  $M_{DB1}$ ,  $M_{DB2}$ ,  $M_{DB3}$ ,  $M_{DB4}$ . Assuming the current through  $M_{DB3}$  ( $M_{DB4}$ ) is  $K_{DB} I_S$ , and the current through  $M_{DB1}$  ( $M_{DB2}$ ) is  $K_{DB} I_S / (K_1 + K_2)$ , the  $SR_G$  is expressed as,

$$SR_G = \frac{(K_1 + K_2)I_B + \frac{K_{DB}}{K_S} I_L}{C_G} \quad (5)$$

In quiescent mode,  $I_S$  is negligible. It increases when load current increases. At full-load condition if the bias current of the EA is increased by a factor of  $K_m$ , the dominant pole  $\omega_{PG}$  and the loop UGB are moved to higher frequencies by  $K_m$  and  $\sqrt{K_m}$  times, respectively; the  $SR_G$  is increased by  $K_m$  times; and the EA DC gain is reduced by  $\sqrt{K_m}$  times. However, the reduction of the EA DC gain is compensated to a certain extent by the increased gain of the NMOS regulation FET.

During load transients when output sees undershoot ( $\Delta V_{OUT}$ ), the transistor  $M_S$  detects the variation at  $V_{OUT}$

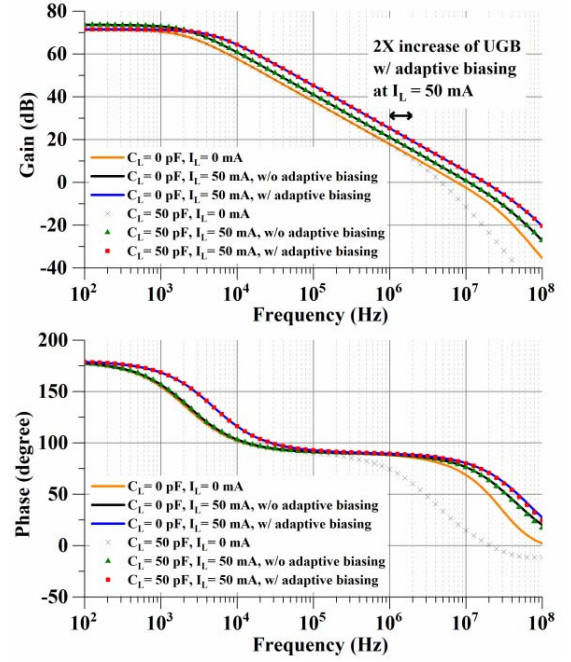


Fig. 2. LDO open-loop gain and phase plots.

and generates a load dependent transient current  $g_{mS} \Delta V_{OUT}$ , where  $g_{mS}$  is load dependent transconductance of  $M_S$ . Through the current mirrors, the ABC enables the tail transistors  $M_{DB1}$ - $M_{DB4}$  to effectively increase the transient bias current of the EA. Hence, the  $SR_G$  is represented as,

$$SR_G = \frac{(K_1 + K_2)I_B + \frac{K_{DB}}{K_S} I_L + K_{DB} g_{mS} \Delta V_{OUT}}{C_G} \quad (6)$$

Therefore, with the adaptive biasing circuit the  $SR_G$  becomes a function of  $I_L$  and transient  $V_{OUT}$  change. As the integrated CPVD supplies the EA output stage bias current change, the  $K_m$  is kept 2 in the design.

### III. SMALL SIGNAL AC ANALYSIS

Small signal AC model of the LDO is approximated by two low frequency poles:  $\omega_{PG}$  at the gate of  $M_N$  and  $\omega_{POUT}$  at the  $V_{OUT}$ . The open loop transfer function of the LDO is written as,

$$H_{LDO}(s) = \frac{G_{mEA} R_{OE} A_{OE} g_{mMN} R_{OUT} \left(1 + \frac{s}{\omega_{ZC}}\right)}{\left(1 + \frac{s}{\omega_{PG}}\right) \left(1 + \frac{s}{\omega_{POUT}}\right)} \quad (7)$$

where,  $\omega_{PG} = 1/R_{OE}(C_G + C_C)$ ,  $\omega_{POUT} = 1/R_{OUT}(C_L + C_P)$ ,  $\omega_{ZC} = 1/R_C C_C$ , and  $C_P$  is a parasitic capacitance at  $V_{OUT}$  that is limited to a few pico-Farad. For OECL-LDOs,  $\omega_{PG}$  is the dominant low frequency pole. The pole  $\omega_{POUT}$  is a function of  $I_L$  (i.e.,  $1/R_L$ ) as shown in (4), and is moved to high frequency when  $I_L$  increases. At no-load or light-load condition, low  $R_{IEA}$  pushes  $\omega_{POUT}$  to high frequency and improves loop phase margin (PM) for zero  $C_L$ . To improve the loop PM at no-load and light-load for 50 pF  $C_L$ , a small series R-C compensation network ( $R_C$  of 5 k $\Omega$  and  $C_C$  of 2 pF) is added at EA output. The other design parameters are:  $I_B = 2.3 \mu A$ ,  $K_1 = 10$ ,  $K_2 = 4$ ,  $K_m = 2$ .

Fig. 2 shows the small-signal AC response of the LDO open-loop at no-load and full-load ( $I_L = 50$  mA), with and without using adaptive biasing along with 0 pF and 50 pF  $C_L$ .



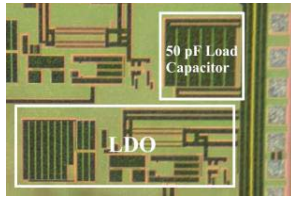


Fig. 3. Die micrograph.

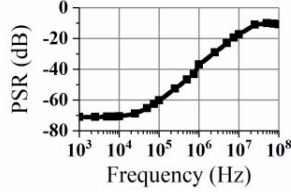
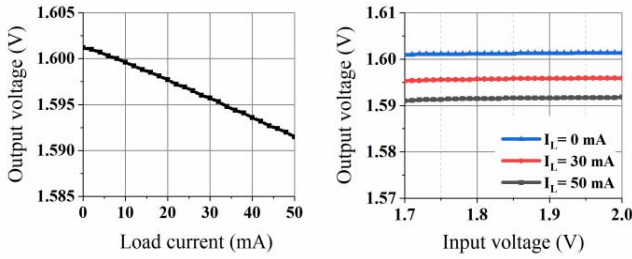
Fig. 4. PSR at  $I_L = 50$  mA.

Fig. 5. Measured DC load and line regulations.

High open-loop DC-gain of 71.5 dB and UGB of 18 MHz at full-load condition are achieved. For a 2X increase of bias current (as  $K_m = 2$ ) in the EA (due to adaptive biasing) at full-load condition, LDO UGB is increased by 2X instead of  $\sqrt{2}X$ , and DC loop gain remains constant instead of decreasing by  $\sqrt{2}X$ . This is due to about  $\sqrt{2}X$  increase of gain at the LDO output regulation stage.

As  $\omega_{PG}$  is the dominant pole in the design, a trade-off exists between the achievable UGB and the  $I_L$  requirement, where the  $I_L$  requirement decides the size of the NMOS regulation FET. Hence, the EA has been designed with required output impedance to achieve the maximum loop UGB ensuring sufficient loop gain to provide a good steady-state regulation.

#### IV. MEASUREMENT RESULTS

The proposed LDO regulator is designed and fabricated in a 0.18  $\mu\text{m}$  CMOS technology and occupies 0.21  $\text{mm}^2$  die area. The die micrograph is shown in Fig. 3. A  $C_L$  of 50 pF capacitor is also integrated on-chip. The implemented LDO provides a regulated  $V_{OUT}$  of 1.4 -1.6 V from a  $V_{IN}$  range of 1.6 -1.8 V with  $V_{DROP}$  of 200 mV across the regulation FET. The measured  $I_Q$  including the CPVD is 133  $\mu\text{A}$ . The DC load and line regulations are measured less than 194  $\mu\text{V}/\text{mA}$  at  $V_{IN} = 1.8$  V, and 2.67 mV/V at  $I_L = 50$  mA as shown in Fig. 5, respectively. The obtained PSR is 71 dB @ 1 kHz as shown in Fig. 4.

Fig. 6 shows the line transient response for 200 mV step in 10 ns edge-time at  $V_{IN} = 1.8$  V. The maximum  $\Delta V_{OUT}$  observed is 36 mV for  $C_L = 0$  pF, and 34 mV for  $C_L = 50$  pF, respectively. The load transient response is measured at  $V_{IN} = 1.8$  V,  $V_{OUT} = 1.6$  V, and edge-time of 350 ps

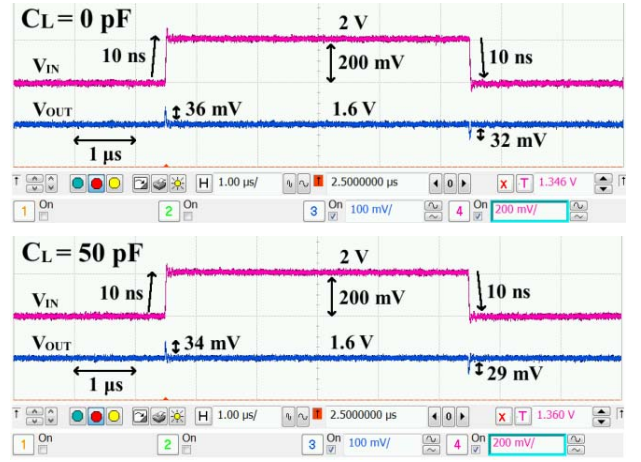
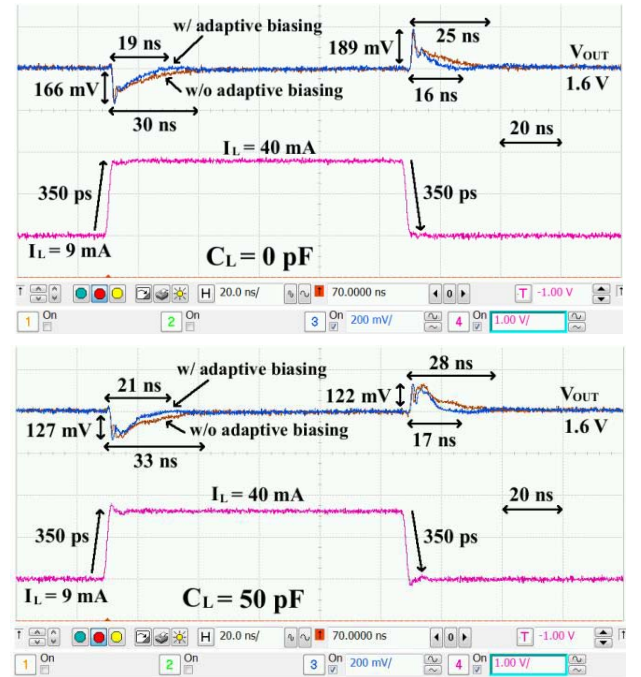
Fig. 6. Measured line transient response at  $I_L = 40$  mA.

Fig. 7. Measured load transient response w/ and w/o adaptive biasing.

for the load step. Fig. 7 shows the load transient response for 4.5X  $I_L$  step between 9 mA and 40 mA. The undershoot voltages ( $\Delta V_{OUT}$ ) are 166 mV and 127 mV for 0 pF and 50 pF  $C_L$  respectively, and overshoot voltages are 189 mV and 122 mV for 0 pF and 50 pF  $C_L$ , respectively. The observed settling times ( $T_{SETTLE}$ ) from undershoot are less than 19 ns and 21 ns for 0 pF and 50 pF  $C_L$ , respectively. The settling times from overshoot are less than 16 ns and 17 ns for 0 pF and 50 pF  $C_L$ , respectively. The figure also shows the load transient response for the same set-up when the adaptive biasing is disabled. After using the adaptive biasing, for low-to-high  $I_L$  step, the  $T_{SETTLE}$  is reduced by 37% and 36% for 0 pF and 50 pF  $C_L$ , respectively. The settling time reduction is 36% and 39%, respectively, for high-to-low  $I_L$  step. Fig. 8 also shows load transient response for  $I_L$  step from no-load condition.

Different performance parameters of the proposed LDO are summarized and compared with state-of-the-art OECL-LDOs designed with different specifications using different technologies in Table I. The edge-time of output load step is one of the

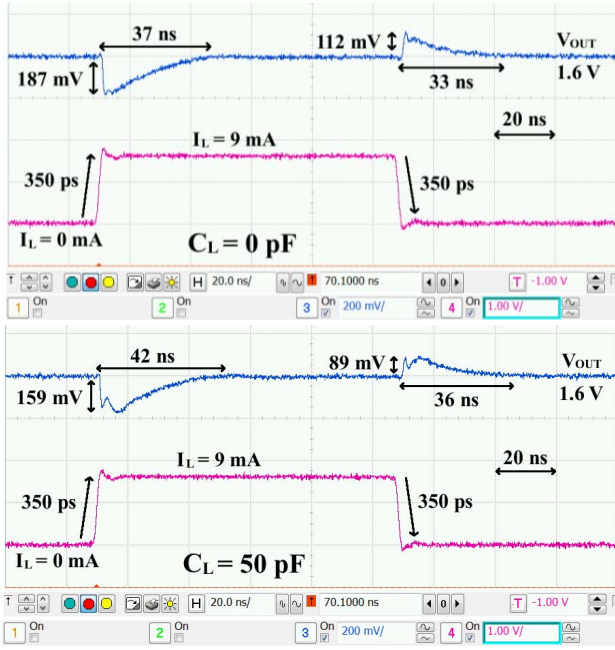


Fig. 8. Measured load transient response for load step from no-load condition.

TABLE I  
PERFORMANCE COMPARISON WITH STATE-OF-THE-ART OECL-LDOs

Parameters	This work	TCAS-I 2017 [8]	TPE 2016 [7]	TCAS-II 2013 [1]	ESSCC 2012 [10]	TCAS-II 2010 [6]
Technology ( $\mu\text{m}$ )	0.18	0.35	0.065	0.11	0.065	0.35
Regulation FET	NMOS	NMOS	NMOS	PMOS	NMOS	PMOS
$V_{IN}$ (V)	1.6-1.8	1.4-2.7	2.4-2.6	1.8-3.8	2.07-5.5	1.8-4.5
$V_{OUT}$ (V)	1.4-1.6	1.2-2.5	1	1.6-3.6	1.3	1.6
Max $I_L$ (mA)	50	1	30	200	200	100
$I_Q$ ( $\mu\text{A}$ )	133	1	161	41.5	176	20
$C_L$ (pF)	0-50	0-1000	30	40	4400	0-100
$\Delta V_{OUT}$ (mV)	166	128	195	385	104	97
$\Delta I_L$ (mA)	31	0.8	30	199.5	149	100
$T_{SETTLE}$ (ns)	19	~10400	~500	650	~60	<9000
PSR (dB) @ Hz	71 @1k	~47 @10k	~40 @10k	NA	50 @1k	40 @10k
Edge time (ns)	0.35	76	0.2	500	16	100
K ratio*	1.75	380	1	2.5k	80	500
FOM (mV) [4]**	1.25	60.80	1.05	200.22	9.83	9.70
FOM <sub>N</sub> (mV/ $\mu\text{m}^2$ )***	38.47	496.33	247.69	16547.05	2326.07	79.18

$$^{**}FOM = K \left( \frac{\Delta V_{OUT} I_Q}{\Delta I_L} \right); \quad ^{***}FOM_N = K \left( \frac{\Delta V_{OUT} I_Q}{\Delta I_L} \right) \frac{1}{L^2};$$

$$^*K = \frac{\Delta t \text{ used in the measurement}}{\text{the smallest } \Delta t \text{ among designs for comparison}}$$

key parameters to determine the load-transient response of the OECL-LDO. Hence, the figure-of-merit (FOM) defined in [4] is used here for the comparison, and the smaller FOM indicates the better performance. If a technology offering a smaller minimum transistor length ( $L$ ) is used, the FOM could be better due to the lower parasitic capacitance of the transistor [5]. Therefore, for fair comparison the FOM should include the parasitic capacitance, which is proportional to transistor area, hence, the square of transistor length ( $L$ ) assuming an identical aspect ratio of the transistor. Therefore, a new FOM (FOM<sub>N</sub>) is

introduced by including  $L^2$  in the denominator of FOM in [4]. The LDO performance is also compared based on FOM<sub>N</sub> as shown in Table I. The FOM of the proposed LDO is smaller than other LDOs excluding FOM in [7], which has used 65 nm technology. However, the smallest FOM<sub>N</sub> of 38.47 mV/ $\mu\text{m}^2$  is achieved for the proposed LDO.

## V. CONCLUSION

A fully-integrated output load capacitor-less NMOS LDO using adaptive biasing designed with cross-coupled common-gate input stage error amplifier is presented. The low output impedance of the NMOS regulation stage and low input impedance of the error amplifier reduces no-load stability issue, and provides a wide LDO bandwidth hence fast load transient response. The direct gate-to-source feedback in NMOS regulation FET and the adaptive biasing further improve load transient response without consuming extra quiescent current. A prototype is designed and fabricated in 0.18  $\mu\text{m}$  CMOS technology for zero-to-50 pF load capacitance. High open-loop DC gain provides accurate load regulation of 194  $\mu\text{V}/\text{mA}$  and line regulation of 2.67 mV/V. The proposed LDO achieves 166 mV undershoot and 19 ns settling time with zero load capacitance for 9 to 40 mA load step in 350 ps edge-time. It consumes 133  $\mu\text{A}$  quiescent current, and achieves the smallest FOM<sub>N</sub> of 38.47 mV/ $\mu\text{m}^2$ .

## REFERENCES

- [1] Y.-I. Kim and S.-S. Lee, "A capacitorless LDO regulator with fast feedback technique and low-quiescent current error amplifier," *IEEE Trans. Circuits Syst. II, Exp. Briefs*, vol. 60, no. 6, pp. 326-330, Jun. 2013.
- [2] X. Qu, Z.-K. Zhou, B. Zhang, and Z.-J. Li, "An ultralow-power fast-transient capacitor-free low-dropout regulator with assistant push-pull output stage," *IEEE Trans. Circuits Syst. II, Exp. Briefs*, vol. 60, no. 2, pp. 96-100, Feb. 2013.
- [3] T. Y. Man, P. K. T. Mok, and M. Chan, "A high slew-rate push-pull output amplifier for low-quiescent current low-dropout regulators with transient-response improvement," *IEEE Trans. Circuits Syst. II, Exp. Briefs*, vol. 54, no. 9, pp. 755-759, Sep. 2007.
- [4] J. Guo and K. N. Leung, "A 6- $\mu\text{W}$  chip-area-efficient output-capacitorless LDO in 90-nm CMOS technology," *IEEE J. Solid-State Circuits*, vol. 45, no. 9, pp. 1896-1905, Sep. 2010.
- [5] S.-W. Hong and G.-H. Cho, "High-gain wide-bandwidth capacitor-less low-dropout regulator (LDO) for mobile applications utilizing frequency response of multiple feedback loops," *IEEE Trans. Circuits Syst. I, Reg. Papers*, vol. 63, no. 1, pp. 46-57, Jan. 2016.
- [6] E. N. Y. Ho and P. K. T. Mok, "A capacitor-less CMOS active feedback low-dropout regulator with slew-rate enhancement for portable on-chip application," *IEEE Trans. Circuits Syst. II, Exp. Briefs*, vol. 57, no. 2, pp. 80-84, Feb. 2010.
- [7] Y. Lu, W.-H. Ki, and C. P. Yue, "An NMOS-LDO regulated switched-capacitor DC-DC converter with fast-response adaptive-phase digital control," *IEEE Trans. Power Electron.*, vol. 31, no. 2, pp. 1294-1303, Feb. 2016.
- [8] S.-Y. Peng, L.-H. Liu, P.-K. Chang, T.-Y. Wang, and H.-Y. Li, "A power-efficient reconfigurable output-capacitor-less low-dropout regulator for low-power analog sensing front-end," *IEEE Trans. Circuits Syst. I, Reg. Papers*, vol. 64, no. 6, pp. 1318-1327, Jun. 2017.
- [9] I. M. Filanovsky, M. Reja, and V. Ivanov, "Structural design of a CMOS full low dropout voltage regulator," in *Proc. IEEE Int. Conf. Electron. Circuits Syst.*, Dec. 2007, pp. 763-766.
- [10] T. Jackum, W. Pribyl, F. Praemassing, G. Maderbacher, and R. Riederer, "Capacitor-less LVR for a 32-Bit automotive microcontroller SoC in 65nm CMOS," in *Proc. IEEE Eur. Solid-State Circuits Conf.*, Bordeaux, France, Sep. 2012, pp. 329-332.
- [11] M. Huang, Y. Lu, S.-P. U, and R. P. Martins, "20.4 An output-capacitor-free analog-assisted digital low-dropout regulator with tri-loop control," in *Proc. IEEE Int. Solid-State Circuits Conf.*, San Francisco, CA, USA, Feb. 2017, pp. 342-343.
- [12] P. Favrat, P. Deval, and M. J. Declercq, "A high-efficiency CMOS voltage doubler," *IEEE J. Solid-State Circuits*, vol. 33, no. 3, pp. 410-416, Mar. 1998.